Biochemistry and Biophysics Reports 38 (2024) 101654

Contents lists available at ScienceDirect

Biochemistry and Biophysics Reports

journal homepage: www.elsevier.com/locate/bbrep

Identification of mitophagy-related hub genes during the progression of spinal cord injury by integrated multinomial bioinformatics analysis☆

Zhihao Guo [a,1], Zihui Zhao [b], Xiaoge Wang [b], Jie Zhou [a], Jie Liu [b,c], Ward Plunet [d], Wenjie Ren [b,c], Linqiang Tian [a,b,c,*]

[a] The Department of Orthopedics, The Third Affiliated Hospital of Xinxiang Medical University, Xinxiang, Henan, China
[b] Institute of Trauma & Orthopedics, The Third Affiliated Hospital of Xinxiang Medical University, Xinxiang, Henan, China
[c] Clinical Medical Center of Tissue Engineering and Regeneration, Xinxiang Medical University, Xinxiang, Henan, China
[d] International Collaboration on Repair Discoveries (ICORD), Blusson Spinal Cord Center, Vancouver, British Columbia, Canada

ARTICLE INFO

Keywords:
Spinal cord injury
Mitophagy
Immune cells
Hub genes
Bioinformatics analysis

ABSTRACT

Spinal cord injury (SCI) is a disturbance of peripheral and central nerve conduction that causes disability in sensory and motor function. Currently, there is no effective treatment for SCI. Mitophagy plays a vital role in mitochondrial quality control during various physiological and pathological processes. The study aimed to elucidate the role of mitophagy and identify potential mitophagy-related hub genes in SCI pathophysiology. Two datasets (GSE15878 and GSE138637) were analyzed. Firstly, the differentially expressed genes (DEGs) were identified and mitophagy-related genes were obtained from GeneCards, then the intersection between SCI and mitophagy-related genes was determined. Next, we performed gene set enrichment analysis (GSEA), weighted gene co-expression network analysis (WGCNA), protein-protein interaction network (PPI network), least absolute shrinkage and selection operator (LASSO), and cluster analysis to identify and define the hub genes in SCI. Finally, the link between hub genes and infiltrating immune cells was investigated and the potential transcriptional regulation/small molecular compounds to target hub genes were predicted. In total, SKP1 and BAP1 were identified as hub genes of mitophagy-related DEGs during SCI development and regulatory T cells (Tregs)/resting NK cells/activated mast cells may play an essential role in the progression of SCI. LINC00324 and SNHG16 may regulate SKP1 and BAP1, respectively, through miRNAs. Eleven and eight transcriptional factors (TFs) regulate SKP1 and BAP1, respectively, and six small molecular compounds target BAP1. Then, the mRNA expression levels of BAP1 and SKP1 were detected in the injured sites of spinal cord of SD rats at 6 h and 72 h after injury using RT-qPCR, and found that the level were decreased. Therefore, the pathways of mitophagy are downregulated during the pathophysiology of SCI, and SKP1 and BAP1 could be accessible targets for diagnosing and treating SCI.

1. Introduction

Spinal cord injury (SCI) caused a total or partial loss of sensory and motor function below the affected region [1]. Approximately 250–500 million individuals suffer worldwide each year, and SCI is a heavy burden for affected patients and their families and generates high health care costs for society [2,3]. The pathophysiology of SCI includes both primary and secondary injury [4]. Primary injury is an immediate injury caused by a mechanical contusion or extrusion. Secondary injuries include tissue edema, inflammatory reaction, necrosis, oxidative stress (OS), mitochondrial dysfunction, and programmed cell death (PCD), leading to tissue damage and inhibition of nerve tissue regeneration in the injury area [5]. Mitophagy has recently attracted increasing attention as a major hurdle for neural regeneration in SCI [6,7]; however, the molecular mechanism remains unclear. Further studies are required to elucidate the underlying molecular mechanisms.

Mitochondrial autophagy, also termed mitophagy, is the process of eliminating damaged/superfluous mitochondria [8] and plays an

☆ Claim: This research received no commercial support and no authors have any financial conflicting interests to disclose.

* Corresponding author. Institute of Trauma and Orthopedics, The third Affiliated Hospital of Xinxiang Medical University, Xinxiang, 453003, China.
E-mail addresses: heartoz@163.com (Z. Guo), wstiansenzhi@126.com (L. Tian).
[1] Mailing address: Department of Orthopedics, The third Affiliated Hospital of Xinxiang Medical University, Xinxiang, 453003, China.

https://doi.org/10.1016/j.bbrep.2024.101654
Received 21 November 2023; Received in revised form 24 January 2024; Accepted 25 January 2024

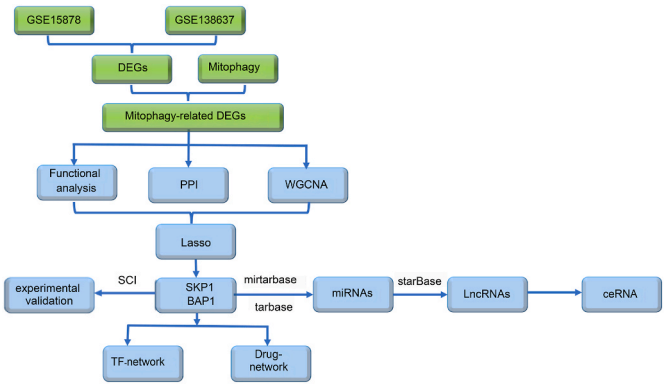

Fig. 1. Flow chart. The flow chart of the data collection and analysis.

essential role in maintaining mitochondrial homeostasis and neuronal cell survival [9]. A previous study found that maltol, a natural antioxidative compound, enhances mitophagy and promotes the recovery of mitochondrial function, which improves locomotor function after SCI [10]. Meng et al. found that rosiglitazone reduced mitophagy and ameliorated the impairment of motor functions in rats with SCI [11]. Mitophagy has excellent potential in the treatment of SCI. Therefore, further research is required to illustrate the mechanisms of mitophagy in SCI.

In this study, we used GSE15878 and GSE138637 datasets to conduct differential gene expression analyses. Then, the datasets from the Gene Expression Omnibus (GEO) and GeneCards were used to identify differentially expressed genes (DEGs) related to SCI mitophagy. Additionally, gene ontology (GO) functional annotation analysis, Kyoto Encyclopedia of Genes and Genomes (KEGG) pathway enrichment analysis, and gene set enrichment analysis (GSEA) were performed. Next, key genes of mitophagy in SCI were identified by weighted gene co-expression network analysis (WGCNA) and least absolute shrinkage and selection operator (LASSO). Transcriptional regulation and possible therapeutic targets were screened by combined bioinformatics analysis and machine-learning techniques. Then, the SCI model of SD rats was building and the mRNA expression level of BAP1 and SKP1 were detected at 6 h and 72 h after injury. The results showed that the BAP1 and SKP1 was decreased at the detection time. We aimed to elucidate the relationship between critical genes and immune cells, transcriptional factors, and drugs to uncover the molecular mechanisms of mitophagy after SCI.

2. Materials & methods

2.1. Data acquisition and DGEs analysis

The gene expression dataset GSE15878 [12] was downloaded from GEO [13] and included 16 SCI samples and 16 normal spinal cord samples. GSE138637 was obtained from GEO and contained four SCI samples and four sham controls.

The limma package [14] in R was applied to obtain different genes according to the grouped information to compare the gene expression levels in the SCI and sham groups. DEGs for each comparison were defined by setting a cutoff adj $P < 0.05$ and absolute value of logFC ≥ 1.

The mitophagy-related gene list was downloaded from the GeneCards database [15]. With the keyword "mitophage," 1903 genes were acquired as mitophagy-related genes. The intersection of DEGs from the GEO database and mitophagy-related genes was used to obtain the mitophagy-related genes in SCI. A Venn diagram was generated using the Venn diagram tool. The protein-protein interactions (PPI) analysis was executed using the Search Tool for the Retrieval of Interacting Genes (STRING) database (STRING v11.0)[14] (https://string-db.org/) and visualized using Cytoscape (version 3.6.1).

2.2. GO and KEGG enrichment analyses of mitophagy-related genes in SCI

GO enrichment analysis [16], including cell composition, biological processes, and molecular functions, is used for large-scale functional enrichment research. The Kyoto Encyclopedia of Genes and Genomes (KEGG)[17] is a extensively used database that stores large amounts of data on genomes, biological pathways, diseases, chemical substances, and drugs. The R package 'clusterProfiler'[18] was used to perform GO and KEGG enrichment analyses of mitophagy-related genes in SCI. Statistical significance was set at $P < 0.05$.

2.3. Gene set enrichment analysis

To uncover the biological differences between the injured and normal spinal cords, the R package 'clusterProfiler' was used to carry out GSEA on the gene expression matrix. Gene set enrichment analysis (GSEA)[19], a computational method that determines whether a pre-defined set of genes demonstrates statistically significant, concordant differences between two biological states, was performed using the gene expression data. The "c2.all.v7.5.2.entrez.gmt" was downloaded from MSigDB database [20] and selected as a reference gene set. GSEA was performed to identify significantly enriched gene sets across GSE15878. A false discovery rate (FDR) < 0.25 and $p < 0.05$ was considered significantly enriched.

2.4. Modules of Co-expressed genes were identified using the WGCNA

A weighted gene co-expression network analysis (WGCNA)[21] was executed to describe the co-expression patterns across all samples in an unbiased way and to cluster genes with a similar expression pattern into modules to identify candidate biomarkers or therapeutic targets according to correlations between intra-gene sets and gene-phenotype data. WGCNA was carried out using an R package "WGCNA" to find modules of highly correlated genes. With a minimum module size of 50 genes, cut height set to 40, softpower set to the best soft-thresholding of 4, a minimum height for merging modules of 0.4, and the minimum distance set to 0.2.

2.5. PPI network construction

The PPI network was constructed by correlating individual proteins, which take part in all the processes throughout life, such as the transmission of biological signals/regulation of gene expression/energy metabolism/regulation of the cell cycle. The STRING [14] a database of known and predicted PPI, was used to build a PPI network for SCI-related DEGs and differentially expressed prognostic genes.

Cytoscape (version 3.6.1)[22], an open-source bioinformatics software, was performed to visualize the PPI network. The top ten hub genes of maximum clade credibility (MCC) in the PPI network were obtained using the cytoHubba plugin [23]. The GOSemSim [24] package in R was used to compute the functional correlation between the hub genes.

2.6. LASSO regression model to construct SCI diagnostic model and screen disease characteristic genes

The LASSO regression characteristics include screening variables and adjusting complexity while fitting a generalized linear model. Through regularization, a shrinkage penalty was introduced to limit the coefficients. The regularization process, which uses the sum of the absolute values of all feature weights, improves the interpretability of the model parameters to some extent. LASSO regularization was executed using the "glmnet" package in R [25,26]. In the process of LASSO regularization, the best model was selected to construct an SCI diagnosis model, and the genes in the model were identified as SCI characteristic genes. The models were validated using ROC curve analysis, performed using the

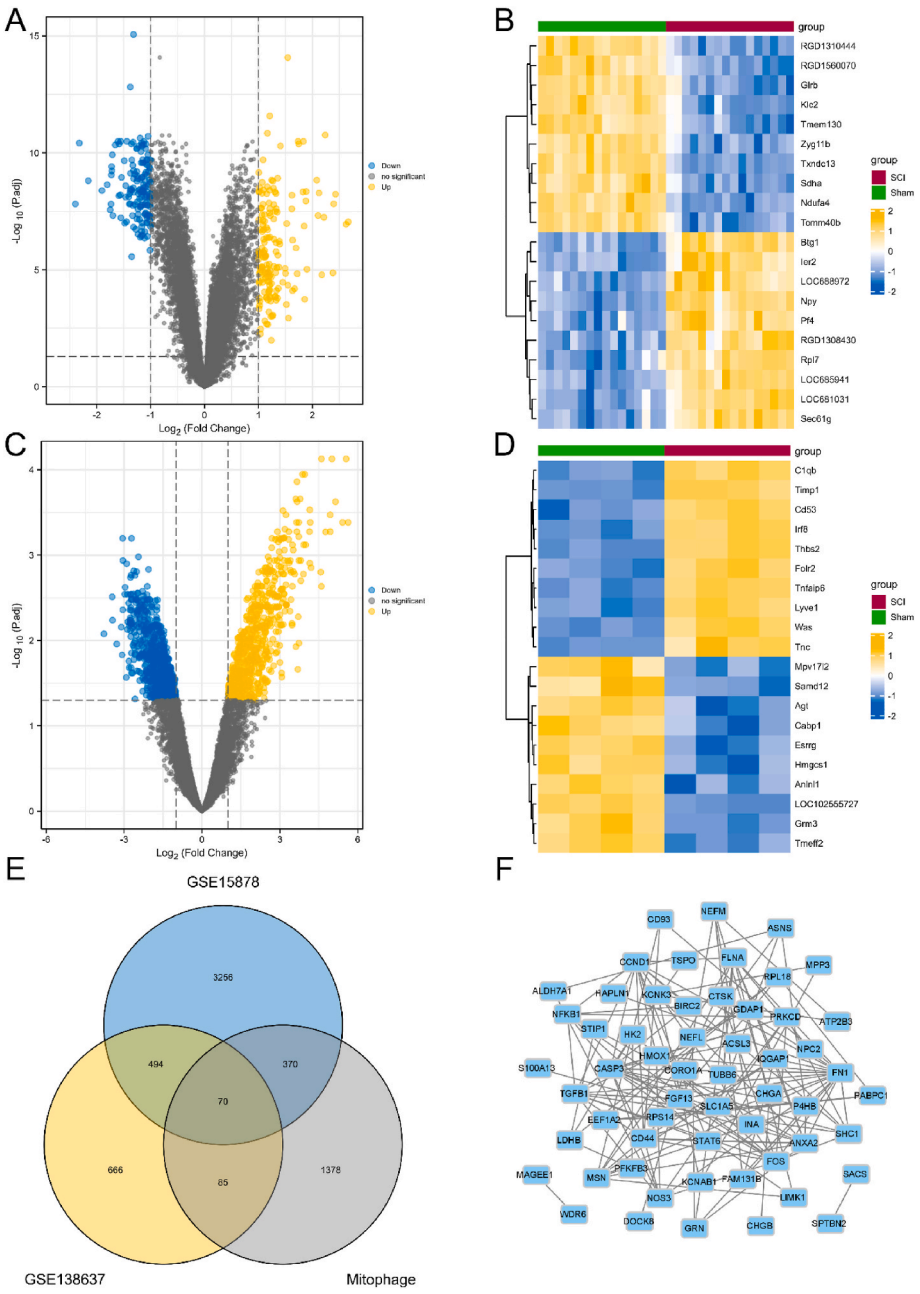

Fig. 2. Identify differently expressed genes. A and C, Volcano plots visualized the fold change and the Adjusted P-value of all genes between the sham and SCI groups in GSE15878 and GSE138637. The X-axis represents fold change, whereas the y-axis represents Adjust P-value, yellow plots were upregulated genes, and blue plots were downregulated genes. B and D, Heatmaps showing DEGs between the sham and SCI groups in GSE15878 and GSE138637, the x-axis represents patient ID, whereas the y-axis represents DEGs. E, Venn diagram indicating the 70 mitophagy-related genes in spinal cord injury identified in GSE15878 (blue circle)/ GSE138637 (blue circle) and mitophagy-related genes (gray circle); F, PPI network 70 mitophagy-related genes in spinal cord injury. (For interpretation of the references to color in this figure legend, the reader is referred to the Web version of this article.)

pROC package in R [27]. Box plots were used to display the differences in characteristic genes between the SCI and normal spinal cord groups.

2.7. Constructing mitophagy-related genes signature in SCI

Consensus clustering, a resampling-based algorithm [28], was used to identify each member and its subgroup number and validate the plausibility of clustering. Consensus clustering was performed based on the mitophagy-related genes previously screened from the GSE15878 and MSigDB databases, and the best cluster was selected using the ConsensusClusterPlus package [29] in R. Different mitophagy patterns were identified according to the results. These genes were identified as hub genes associated with mitophagy.

2.8. Immune infiltration analysis

CIBERSORT(https://cibersort.stanford.edu/) is a deconvolution algorithm that quantifies immunological characteristics based on gene expression signatures using linear support vector regression [30]. The infiltration levels of immune cells were analyzed between injured spinal cord tissue and normal control tissues using the CIBERSORT algorithm based on RNA-Seq data. A differentially enriched composition of infiltrating immune cells was identified in the GSE15878 dataset. Pearson's correlation coefficients were calculated to examine the relationship

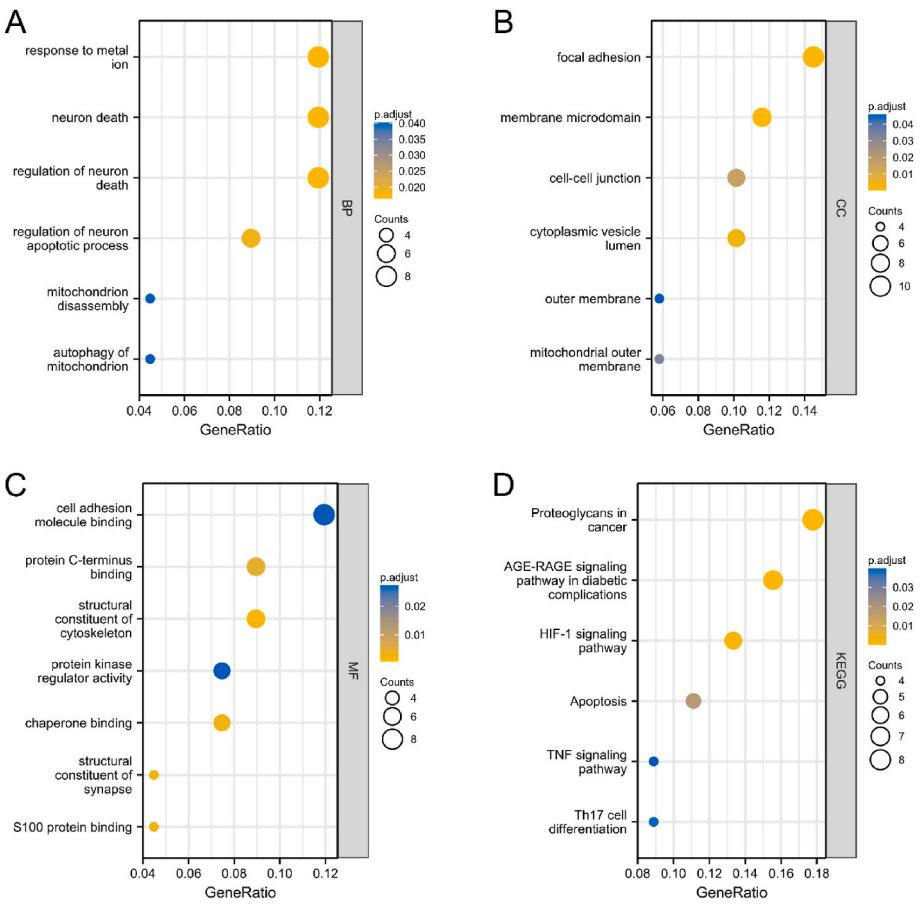

Fig. 3. GO and KEGG enrichment analysis. A–C: GO enrichment analysis (BP, CC, and MF) of 70 mitophagy-related genes in spinal cord injury; D: KEGG pathway enrichment analysis of 70 mitophagy-related genes in spinal cord injury. Abbreviations: BP, biological process; CC, cellular component; MF, molecular function.

between the expression profiles of mitophagy-related genes and immune cells. Furthermore, the study assessed the correlation between mitophagy-related genes and the level of immune infiltration.

2.9. Construction of lncRNAs-miRNAs-mRNAs regulation network

MiRNAs and lncRNA (long non-coding RNA) are important in regulating transcriptional and post-transcriptional gene expression. The miRTarBase database (https://mirtarbase.cuhk.edu.cn/), which collects miRNA-target relationships (MTI, microRNA-target interactions) supported by experimental evidence [31], includes more than 8500 experimentally supported articles on miRNA-target interactions. The TarBase database is a miRNA-target gene database supported by experimental evidence [32]. The miRTarBase and TarBase databases were used to predict the interacting miRNAs of the hub genes, and the intersection was determined.

StarBase [33] was employed to predict miRNA-interacting lncRNAs. The interaction was constructed and visualized using Cytoscape, and it was showed with a Sankey diagram.

2.10. Construction of lncRNAs-miRNAs-mRNAs regulation network

NetworkAnalyst, an online visualization platform for gene expression and meta-analysis database [34], which can perform alignment/-quantification/different gene expression and enrichment/protein interaction analysis, can also search for transcriptional factor regulatory networks. Transcriptional factors bound to the human homologs of mitophagy-related hub genes were predicted and visualized using the NetworkAnalyst (https://www.NetworkAnalyst.ca/) database. Additionally, small-molecule compounds or potential drugs that interact with the mitophagy-related hub genes were predicted using the Drug-Gene Interaction Database (DGIdb) (version 3.0.2, https://www.dgidb.org) and visualized using Cytoscape software Drug-Gene Interaction Network [35].

2.11. Validation experiments

2.11.1. Establishment of SCI in rats

15 Sprague-Dawley rats, aged 6–7 weeks, were purchased from Beijing Vital River Laboratory Animal Technology Co., Ltd. (Beijing, China, SCXK(E)2022–30030) and were randomly divided into the following three groups: sham group, 6 h after SCI and 72 h after SCI. The proceed of contusion SCI model was as followed: After anesthesia by isoflurane, rat was fixed and the laminectomy was performed at the T9-T10 level to expose the spinal cord beneath the dura mater. The Allen methods were used to perform the spinal cord contusion on the back surface of the spinal cord by using 10 g × 50 mm [36]. The lower limb constructions and the tail swing was used as the indicator of successful building of the SCI model. The rats in sham group just perform the laminectomy without weight drop injury. Then the incision was sutured. Bladders of all rats that underwent SCI were emptied manually thrice a day. After stripping blood vessels and spinal meninges, the spinal cord tissue was obtained.

2.11.2. RNA extraction and quantitative real-time polymerase chain reaction (qRT-PCR)

To determine the abundance of BAP1 and SKP1 mRNA, total RNA from the injured spinal cord was extracted using TRIzol and cDNA were synthesized by reverse transcription using a First Strand cDNA synthesis kit (Japan Takara). The expression levels of mRNA were semi-quantified

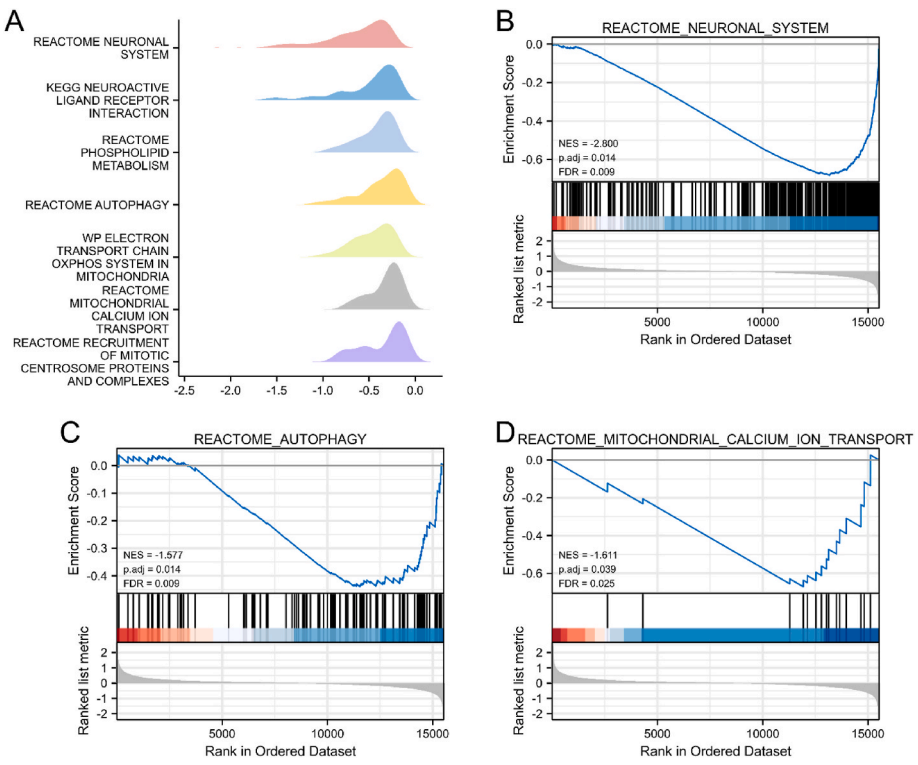

Fig. 4. GSEA analysis. A: GSEA analysis in the GSE15878 data, the x-axis represents the gene ratio, while the y-axis represents the GO terms, and the mountain map visually illustrates the number of genes in each GO term. B–D: GSEA analysis showing the results of the analysis of the neuronal system, autophagy, and mitochondrial calcium ion transport pathways.

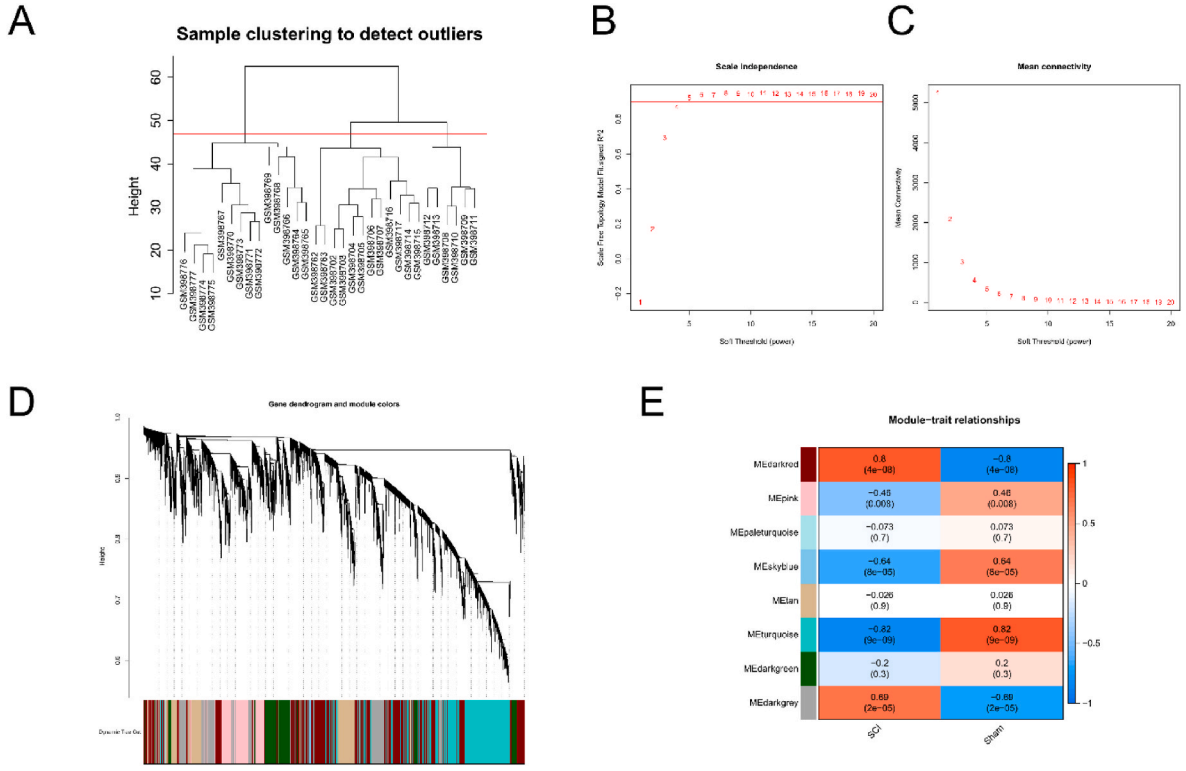

Fig. 5. Identification of co-expression modules in DEGs by WGCNA. A: No outlier samples were found by cut-off height; B, C: Determination of the optimal soft power threshold; D: Dendrogram obtained by hierarchical clustering of genes according to their topological overlap is shown at the top. E: The correlation between modularity genes and spinal cord injury.

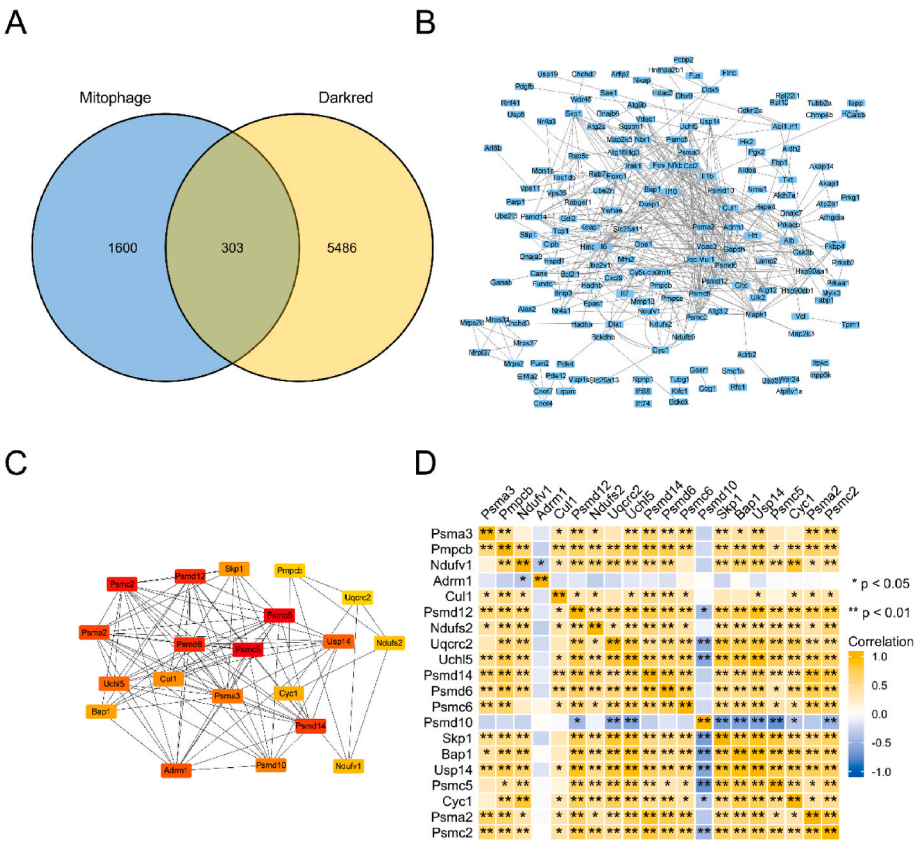

Fig. 6. Protein-protein interaction network. A: The blue circles represent mitophagy-related genes, and the yellow circles represent the Darkred module genes analyzed by WGCNA. Take the intersection to obtain the genes related to mitophagy and spinal cord injury. B: The PPI network of spinal cord injury-related mitophagy genes. C: Top 20 genes in maximum correlation criterion (MCC) screened by cytoHubba. D: Heatmap of correlation coefficients of Hub genes. (For interpretation of the references to color in this figure legend, the reader is referred to the Web version of this article.)

using the real-time polymerase chain reaction by the SYBR Green Master mix and calculated by the $2^{-\Delta\Delta Ct}$ method with normalized to the expression levels of β-actin. Primers used are listed as follows: β-actin, forward: 5′-TGT CAC CAA CTG GGA CGA TA-3′, β-actin, reverse: 5′-GGG GTG TTG AAG GTC TCA AA-3’; SKP1, forward:5′-ATT AAG GGG AAA ACG CCT GAG GAG-3’; SKP1, reverse: 5′-ACT TCT CTT CAC ACC ACT GGT TCT C-3’; BAP1, forward:5′-CCA GCC AGC AGC AAG TCT CC-3’; BAP1, reverse: 5′-CAC GAA CCA GCC ACC TCC TC-3’.

2.11.3. Ethical statement

Experiments were performed under a project license (No. k2023-52-01) granted by institutional ethics board of the Third Affiliated Hospital of Xinxiang Medical University, in compliance with the Third Affiliated Hospital of Xinxiang Medical University guidelines for the care and use of animals.

2.11.4. Statistical analysis

All statistical analyses were conducted using R (https://www.r-project.org/, version 4.0.2). To compare continuous variables between the two groups, the Student’s t-test (normal distribution) or Mann-Whitney test (non-normal distribution) was used to compare differences. All tests were 2-sided with $P < 0.05$ indicating statistical significance.

3. Results

A flow chart illustrating the study process is presented in Fig. 1.

3.1. Analysis of differential gene expression

The DEGs between injured and normal spinal cord tissues were analyzed using the limma package in R and are shown by volcano plots. There were 4190 DGEs and 1315 DGEs in GSE15878 and GSE138637, including 1879 upregulated genes and 2311 downregulated genes in GSE15878 (Fig. 2A) and 633 upregulated genes and 682 downregulated genes in GSE138637 (Fig. 2C), respectively, which differentiated the injured and normal spinal cord tissues (Fig. 2B and D). A total of 70 genes overlapped between DGEs in GSE15878/GSE138637 and mitophagy-related genes (Fig. 2E). PPI analysis revealed interactions between these genes (Fig. 2F).

3.2. Functional enrichment analysis

In the biological process (BP) category, the DEGs are involved in the regulation of neuron death, neuron death, response to a metal ion, regulation of the neuronal apoptotic process, autophagy of mitochondria, and mitochondrial disassembly (Fig. 3A). In the cellular component (CC) category, the DEGs are involved in focal adhesion, membrane microdomain, cytoplasmic vesicle lumen, cell-cell junction, mitochondrial outer membrane, and outer membrane (Fig. 3B). In the molecular function (MF) category, the DEGs were involved in the structural constituents of cytoskeleton, S100 protein binding, structural constituent of synapse, chaperone binding, protein C-terminus binding, cell adhesion molecule binding, and protein kinase regulator activity (Fig. 3C). In the KEGG pathway enrichment analysis, the DEGs were enriched in the AGE-RAGE signaling pathway in diabetic complications, proteoglycans in cancer, HIF-1 signaling pathway, apoptosis, Th17 cell differentiation, and the TNF signaling pathway (Fig. 3D).

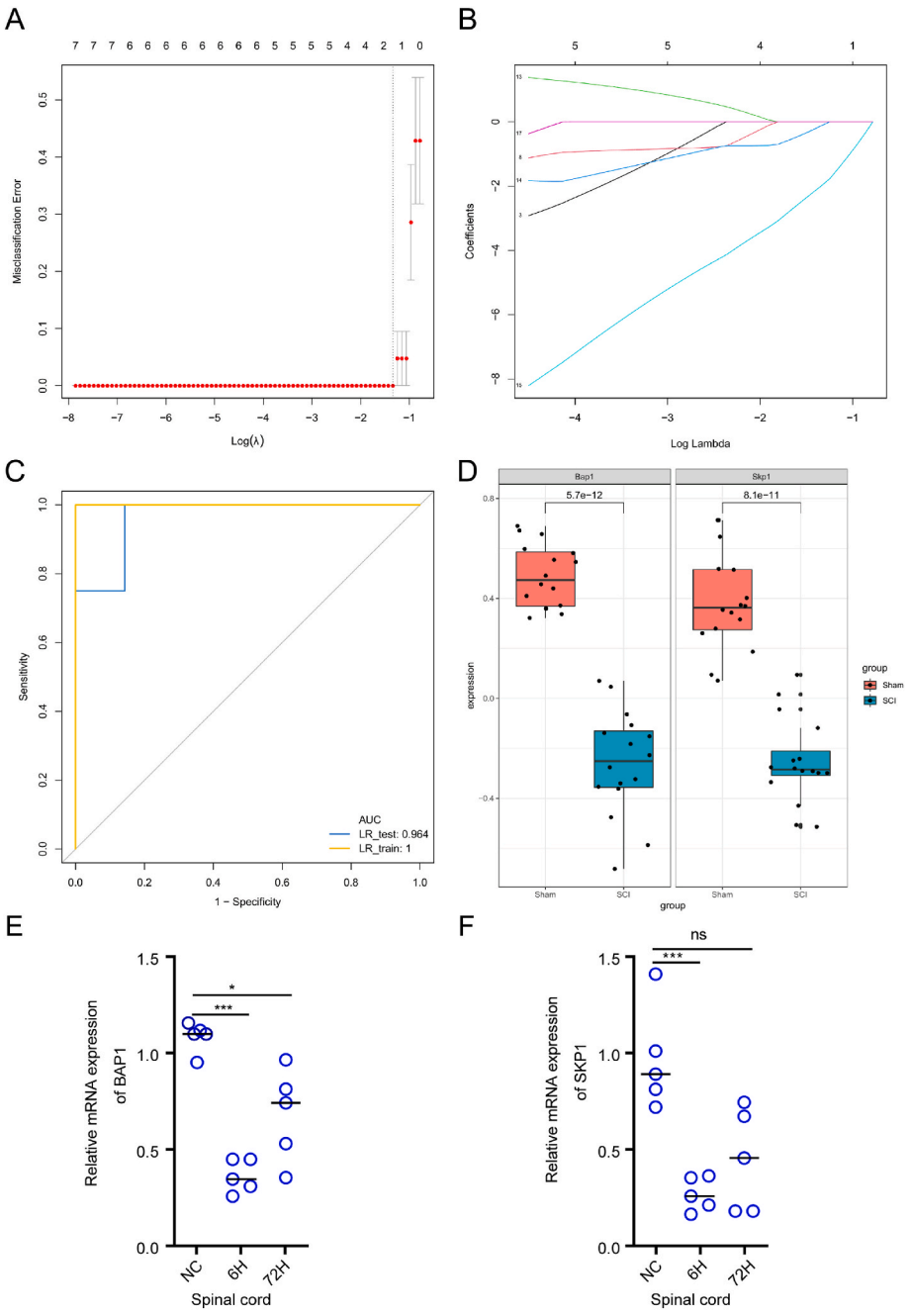

Fig. 7. Construction and validation of LASSO regression diagnostic model. A: Obtaining the best model and the simplest model of LASSO regression; B: The relationship between the selected features and the absolute value of the coefficient; C: The validation of the model by the Train group and the Test group; D: The spinal cord injury group and the normal spinal cord group, characteristics Gene expression is different and the difference is statistically significant; E and F: the mRNA expression level of BAP1 and SKP1 at 6 h and 72 h after SCI in SD rats (n = 5, ***, $P < 0.001$; *, $P < 0.05$; ns, $P > 0.05$) .

3.3. GSEA enrichment analysis

GSEA enrichment pathways (adj *P*-value<0.05) were mainly involved in the neuronal system, neuroactive ligand-receptor interaction, phospholipid metabolism, autophagy, electron transport chain OXPHOS system in mitochondria, mitochondrial calcium ion transport, and recruitment of mitotic centrosome proteins and complexes (Fig. 4A–D).

3.4. Identification of Co-expression modules in DEGs by WGCNA

The co-expression modules were identified using WGCNA between the SCI and control groups. No outlier samples were found when the cut height was set during WGCNA (Fig. 5A). Using the scatter plot, the optimal threshold was set to 4 in the follow-up study (Fig. 5B and C). Co-expression genes in the two groups were clustered in the MEdarkred, MEskyblue, and MEturquoise modules (Fig. 5D). The correlations between modules and SCI were identified based on the gene expression patterns and grouped information. The MEdarkred module, positively correlated with SCI and $p < 0.05$, was selected in the follow-up study (Fig. 5E).

3.5. Protein-protein network analysis

By overlapping genes in the MEdarkred module and mitophagy-related genes (Fig. 6A), the genes associated with SCI were identified.

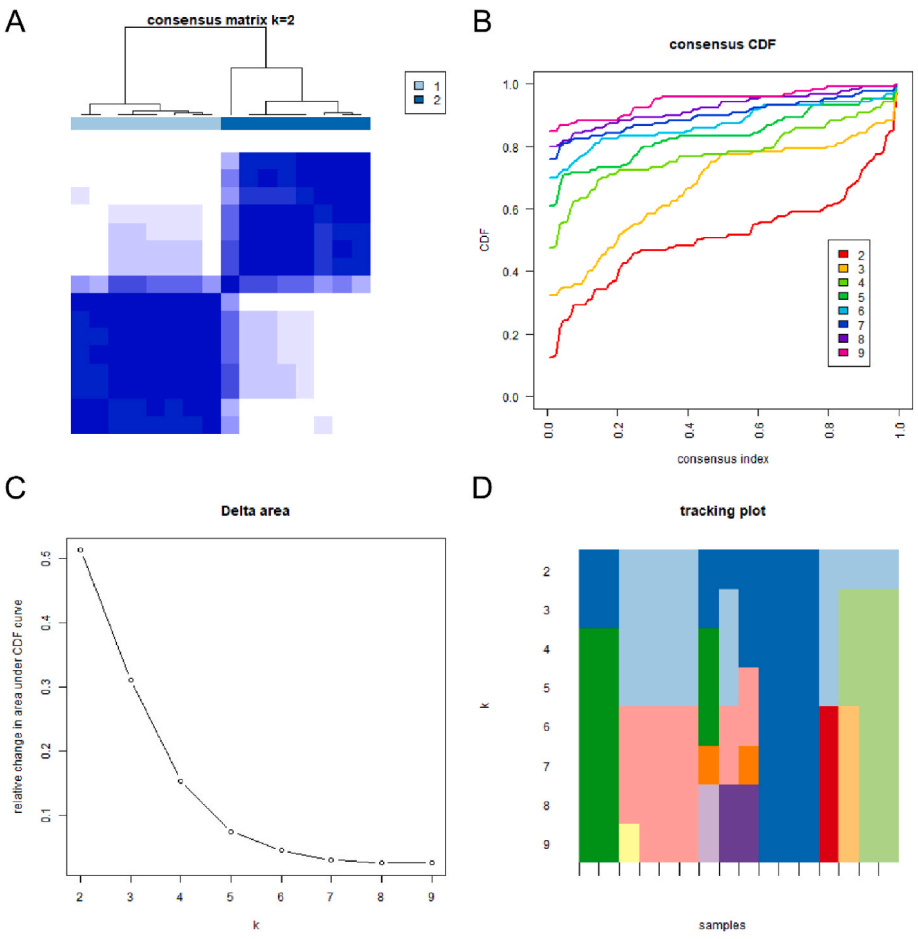

Fig. 8. Consistent cluster analysis of eigengenes in spinal cord injury patients. A: Consistent clustering plot when k = 2; B: Relative change of area under the CDF curve from k = 2 to 9; C: Cumulative distribution function of consistent clustering; D: tracking plot.

The PPI network was then constructed and visualized using Cytoscape (Fig. 6B). The top 20 hub genes selected from the PPI network using the MCC algorithm of the cytoHubba plugin were Psma3, Pmpcb, Ndufv1, Adrm1, Cul1, Psmd12, Ndufs2, Uqcrc2, Uchl5, Psmd14, Psmd6, Psmc6, Psmd10, SKP1, BAP1, Usp14, Psmc5, Cyc1, Psma2, and Psmc2 (Fig. 6C). Pearson correlation coefficients were calculated between the 20 hub genes and were displayed on a colored heat map (Fig. 6D).

3.6. Constructing diagnostic model and identifying signature genes by LASSO regression

LASSO regression was employed to construct a prognostic model by randomly dividing GSE15878 into the training group (used to construct the model) and the test group (used to verify the model) according to 2:1 to identify the signature genes of SCI. During model building, as λ increased, the enrolled characteristic parameters decreased, and the absolute value of the coefficient increased (Fig. 7A and B). We created a prognostic-related risk model that included two genes, SKP1 and BAP1. Then, the prognostic model was validated in the training and test groups by analyzing the ROC curves. In the ROC curve analysis, the area under the curve (AUC) values in the training and the test groups were 1 and 0.964, respectively (Fig. 7C). Signature genes were analyzed in the SCI and sham groups and visualized using a box plot (Fig. 7D). The mRNA expression level of BAP1and SKP1 were decreased at 6 h and 72 h after injury in the SCI model of SD rats (Fig. 7E and F), however there in no significant difference of SKP1 at 72 h between sham and SCI groups.

3.7. Two distinct mitophagy patterns identified by signature genes

The consensus clustering was used for clustering analysis based on two mitophagy-related genes with the “Consensus Cluster Plus” package in R software. Two clusters were identified through consensus clustering with the optimal total cluster number set to k = 2 (Fig. 8A), and the relative change in area under the CDF curve was obtained when k ranged from 2 to 12 (Fig. 8B), the delta area (Fig. 8C), and the tracking plot (Fig. 8D) were acquired.

3.8. Immune infiltration analysis

To evaluate the degree of immune cell infiltration in the SCI and sham groups, the CIBERSORT algorithm was carried out to quantify the degree of infiltration of 22 types of immune cells in GSE15878 (Fig. 9A). A total of 13 types of immune cells showed significant differences in expression between SCI and sham tissues in GSE15878 (Fig. 9B), including B cells, naïve memory B cells, resting memory $CD4^+$ T cells, plasma cells, follicular helper T cells, gamma delta T cells, regulatory T cells (Tregs), resting NK cells, activated NK cells, resting and activated mast cells, eosinophils and neutrophils. The correlation between two mitophagy-related genes (SKP1 and BAP1) and 22 types of immune cells was analyzed. SKP1 was significantly correlated with RNA abundance of activated mast cells and BAP1 with RNA abundance of regulatory T cells (Tregs), activated mast cells, and resting NK cells in GSE15878 ($P < 0.05$) (Fig. 9C).

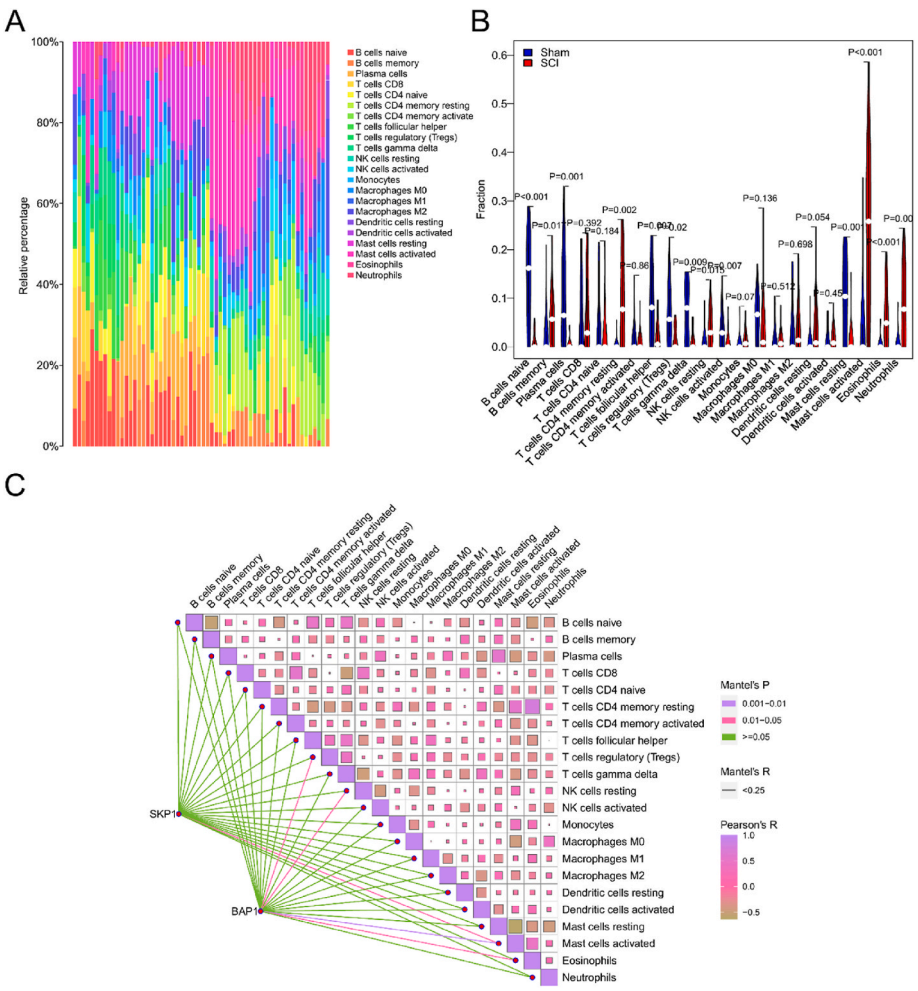

Fig. 9. Immune infiltration analysis. A: Differences in the enrichment abundance of 22 immune cells in the GSE15878 dataset. B: Differences in the enrichment abundance of 22 types of immune cells in the GSE15878 dataset, blue represents normal tissue, red represents spinal cord injury tissue, the X-axis represents 22 types of immune cells, and the Y- axis represents immune cell infiltration abundance. C: Correlation heat map of 22 immune cells and their correlation with hub-mRNA. (For interpretation of the references to color in this figure legend, the reader is referred to the Web version of this article.)

3.9. Constructing hub-mRNA, hub-miRNA, hub-LncRNA interaction network

A lncRNA-miRNA-mRNA interaction network was constructed, which included two mitophagy-related genes, BAP1 and SKP1. The miRTarBase and TarBase databases were used to predict miRNAs interacting with mitophagy-related genes, and there were eight groups of interactions in the intersection set (Fig. 10A). The lncRNAs interacting with miRNAs were predicted using the StarBase database, and a Sankey diagram (Fig. 10B) and network diagram (Fig. 10C) of the lncRNA-miRNA-mRNA network were constructed.

3.10. Hub-TF, hub-drugs regulatory network

The NetworkAnalyst database was employed to construct the mRNA-TF network of mitophagy-related hub genes (Fig. 11A and B). In addition, six small-molecule drugs were found to modulate BAP1 by exploring the Drug-Gene Interaction Database (DGIdb) (Fig. 11C).

4. Discussion

SCI disrupts communication between supraspinal centers and spinal circuits, frequently resulting in permanent functional deficits [37]. There are no effective therapeutic approaches for SCI, as the pathophysiologic mechanisms are still not fully elucidated. Current research shows that mitophagy plays an essential role in SCI development. However, the hub genes and their regulation remain unclear. In this study, we aimed to uncover the hub genes of mitophagy related to SCI for pharmacological intervention, which will improve therapeutic options for SCI.

Based on GEO datasets, GSE15878 and GSE138637 were included in this study. Based on GeneCards datasets, 1903 mitophagy-related genes were acquired. Seventy mitophagy-related genes have been identified in SCI. Functional enrichment and KEGG pathway analyses of the DEGs were carried put. We found a potential association between neural function and death (e.g., response to metal ions, neuronal death, regulation of neuronal cell death, and apoptosis). Next, the top six pathways were screened according to the P-value. The HIF-1 pathway promotes functional restoration after SCI [38] as confirmed by other studies [39, 40].

GSEA results showed that autophagy-related pathways, such as autophagy and mitochondrial calcium ion transport, were down-regulated in SCI. Autophagy promotes neuronal cell survival through apoptosis by releasing energy substrates via degradation of cellular constituents [41,42]. Mitophagic activity is likely required to eliminate ROS accumulation and inhibit pyroptosis after SCI [43]. Impairment of autophagy is a disadvantage in the recovery of neuronal function. The results showed that neuronal cell dysfunction aggravated SCI and promoted neuronal cell death.

The signature genes SKP1 and BAP1were identified and validated in

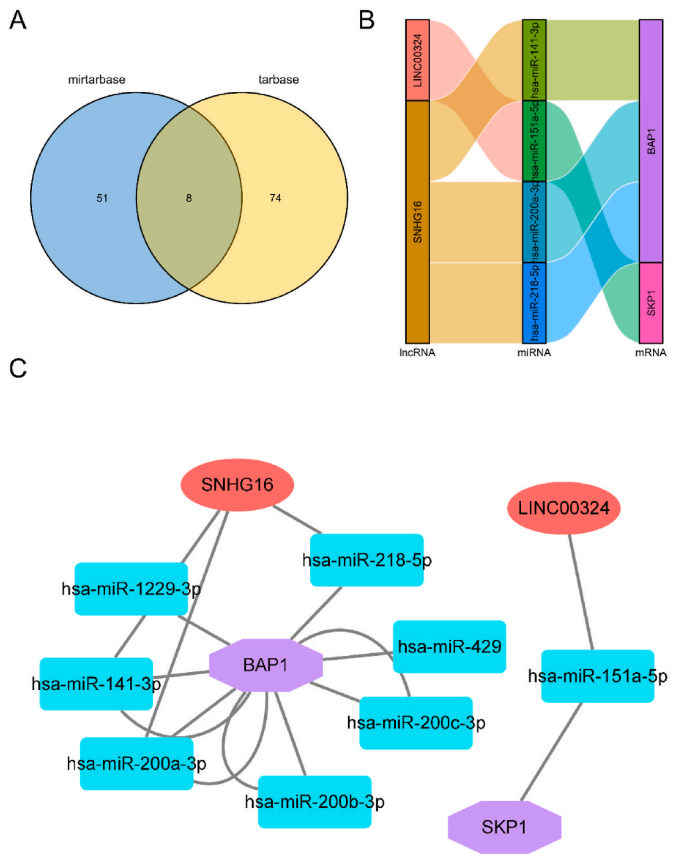

Fig. 10. Construction of hub-mRNA, hub-miRNA, and hub-LncRNA interaction network. A, Venn diagram shows the predicted miRNAs interacting with hub-mRNA based on miRTarBase and TarBase databases. There are 14 groups of interactions in the intersection. B, C: lncRNAs interacting with miRNAs were predicted using the StarBase database, and Sankey diagrams and network diagrams of LncRNA-miRNA-mRNA networks were drawn.

this study. SKP1, a part of the E3 ubiquitin ligase complex that leads to protein degradation, plays an important role in maintaining genome and chromosome stability [44,45]. It is downregulated in the brains of patients with sporadic Parkinson's disease (PD) and plays a neuroprotective role in the adult brain [46]. In our study, we found that SKP1 was downregulated in SCI. BRCA1-associated protein 1 (BAP1) is a ubiquitin C-terminal hydrolase domain-containing deubiquitinase with tumor-suppressor activity [47,48]. Intact BAP1 catalytic activity could increase aerobic glycolysis and lactate secretion and reduce mitochondrial respiration and ATP production [49]. Glycosylation of BAP1 controls the self-renewal of hematopoietic stem cells and hematopoiesis [50]. A recent study showed that BAP1 is essential for commitment to ectoderm, mesoderm, and neural crest lineages during embryonic development [51]. The expression of BAP1 is also downregulated in SCI. In the SCI model of SD rat, the mRNA expression level of BAP1 was reduced compared with sham group at 6 h and 72 h after injury and SKP1 was reduced at 6 h, but there was no significant difference at 72 h compared with sham group. However, the role of SKP1 and BAP1 in SCI development of SCI needs further research.

The immune response plays an important role in maintaining spinal cord homeostasis. Owing to the dysregulated vegetative innervation of the lymphatic and hypothalamic–pituitary–adrenal (HPA) axes, SCI is associated with immune depression syndrome [52,53]. Studies have found that BAP1 is critical for T cell development at several stages [54] and maintaining hematopoietic stem cells and B lymphopoiesis. Mice lacking BAP1 in bone marrow mesenchymal stromal cells show aberrant differentiation of hematopoietic stem and progenitor cells, impaired B lymphoid differentiation, and expansion of myeloid lineages [55]. In our study, we found that regulatory T cells (Tregs) and resting NK cells were upregulated, which may be associated with chronic inflammation. Activated mast cells are positively regulated in SCI, and further research is required to uncover the potential mechanisms.

The transcriptional regulation and potential target compounds of SKP1 and BAP1 were investigated as signature genes. We predicted that lncRNA LINC00324 and small nucleolar RNA host gene 16 (SNHG16) regulate BAP1 and SKP1 through miRNAs. LINC00324 is an autophagy-related long non-coding RNA that can be used as a liquid biopsy marker for esophageal squamous cell carcinoma [56]. In patients with intervertebral disk degeneration (IDD), LINC00324 is upregulated and correlated with IDD development [57]. SNHG16 levels were lower in acute ischemic stroke patients than in controls, negatively correlated with inflammatory cytokines (TNF-α, IL-6) and adhesion molecule ICAM-1, and positively correlated with IL-10 [58]. It was found that over-expressed SNHG16 enhanced cell proliferation and inhibited apoptosis in oxygen-glucose deprivation- and reoxygenation-induced cells and hydrogen peroxide-induced cell injury [59–61]. Our study is the first to predict the roles of LINC00324 and SNHG16 in the development of SCI. Second, we found that there are 11 and 8 TFs regulating the hub genes SKP1 and BAP1, respectively, using the NetworkAnalyst database. Finally, based on the DGIdb database, we found that histone deacetylase inhibitors, such as vorinostat [62], panobinostat [63,64], mTOR pathway inhibitor everolimus [65], apitolisib [66,67], tyrosine kinase inhibitor sunitinib [68] and poly (ADP-ribose) polymerase inhibitor olaparib [69] may target the BAP1 gene and promote neural recovery after SCI.

Our study has several limitations. Firstly, the data in this study were obtained from public sources, which have limitations in terms of statistical imperfection and limited samples; and the two datasets were derived from different strains of rats, so there are some genetics and physiological differences, which may lead to skewed interpretations. Secondly, also we validated the two hub genes SKP1and BAP1, there are also need further studies to evaluate the key pathways and transcriptional regulation and potential target compounds of hub genes involved in SCI development. Thirdly, further research is required to confirm the therapeutic effects of small-molecule compounds in SCI. Therefore, confirmatory experiments were conducted to validate the regulation of transformation during SCI, and the therapeutic effect was evaluated.

5. Conclusions

In this study, mitophagy-related hub genes SKP1 and BAP1 were predicted by bioinformatics and validated by qPCR, then regulatory relationships about non-coding RNAs/TFs/compounds were predicted. Our present study paves the way for future studying the functional role of SKP1 and BAP1 in SCI.

Funding

This study was supported by the Open Project Program of the Third Affiliated Hospital of Xinxiang Medical University (No. KFKTYB202110 and No. KFKTZD202104).

Declaration of generative AI in scientific writing

During scientific writing, there was not used the AI.

Ethics approval and consent to participate

Experiments were performed under a project license (No. k2023-52-01) granted by institutional ethics board of the Third Affiliated Hospital of Xinxiang Medical University, in compliance with the Third Affiliated Hospital of Xinxiang Medical University guidelines for the care and use of animals.

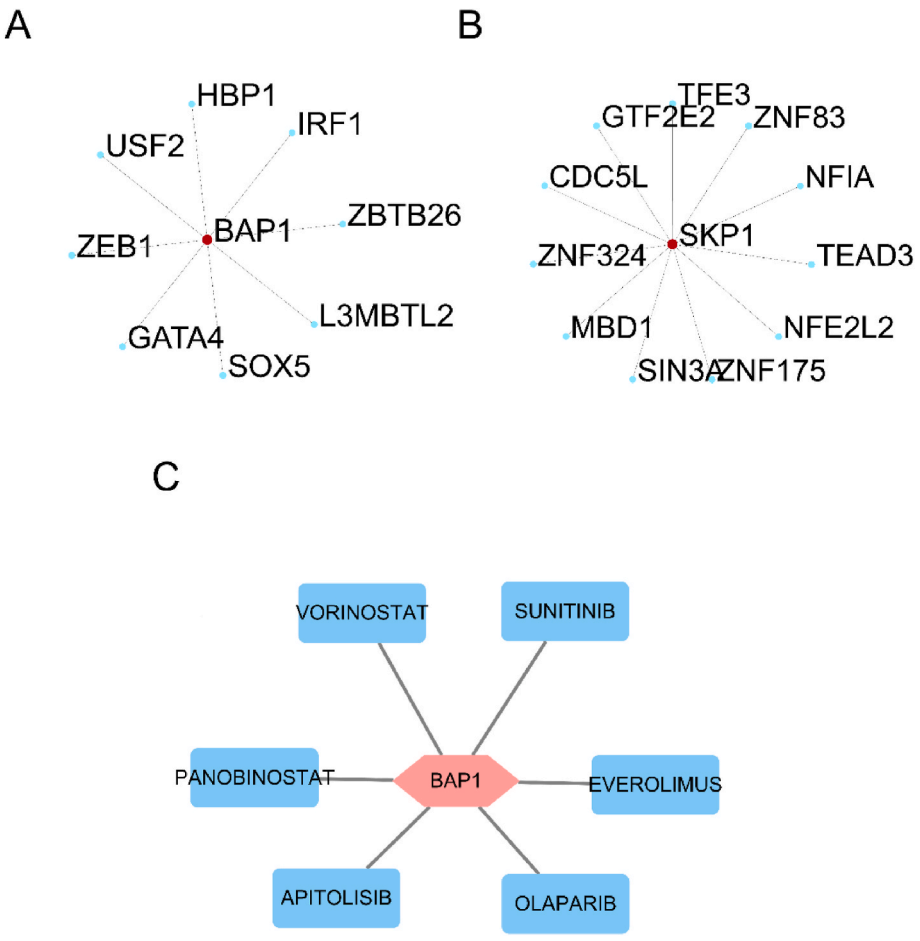

Fig. 11. Hub-TF, hub-drugs regulatory network. A, B: The hub-TF regulatory network analyzed by the NetworkAnalyst database; C: The hub-drugs regulatory network analyzed by the DGIdb database.

Consent for publication

Not applicable.

CRediT authorship contribution statement

Zhihao Guo: Data curation. **Zihui Zhao:** Data curation. **Xiaoge Wang:** Data curation. **Jie Zhou:** Methodology. **Jie Liu:** Conceptualization. **Ward Plunet:** Methodology, Formal analysis. **Wenjie Ren:** Writing – review & editing, Data curation. **Linqiang Tian:** Writing – original draft.

Declaration of competing interest

The authors declare that they have no known competing financial interests or personal relationships that could have appeared to influence the work reported in this paper.

Data availability

Data will be made available on request.

Acknowledgments

The authors are grateful for the financial support from the Third Affiliated Hospital of Xinxiang Medical University. The authors also thank GEO databases for the availability of the data.

References

[1] N. Lago, B. Pannunzio, J. Amo-Aparicio, R. López-Vales, H. Peluffo, Cd200 modulates spinal cord injury neuroinflammation and outcome through cd200r1, Brain Behav. Immun. (2018), https://doi.org/10.1016/j.bbi.2018.06.002.
[2] A. Anjum, M. Yazid, M. Fauzi Daud, J. Idris, A. Ng, A. Selvi Naicker, O. Ismail, R. Athi Kumar, Y. Lokanathan, Spinal cord injury: pathophysiology, multimolecular interactions, and underlying recovery mechanisms, Int. J. Mol. Sci. (2020), https://doi.org/10.3390/ijms21207533.
[3] A. Golestani, P. Shobeiri, M. Sadeghi-Naini, S. Jazayeri, S. Maroufi, Z. Ghodsi, M. Dabbagh Ohadi, E. Mohammadi, V. Rahimi-Movaghar, S. Ghodsi, Epidemiology of traumatic spinal cord injury in developing countries from 2009 to 2020: a systematic review and meta-analysis, Neuroepidemiology (2022), https://doi.org/10.1159/000524867.
[4] V. Vacca, L. Madaro, F. De Angelis, D. Proietti, S. Cobianchi, T. Orsini, P. Puri, S. Luvisetto, F. Pavone, S. Marinelli, Revealing the therapeutic potential of botulinum neurotoxin type a in counteracting paralysis and neuropathic pain in spinally injured mice, Toxins (2020), https://doi.org/10.3390/toxins12080491.
[5] Y. Chen, S. Liu, J. Li, Z. Li, J. Quan, X. Liu, Y. Tang, B. Liu, The latest view on the mechanism of ferroptosis and its research progress in spinal cord injury, Oxid. Med. Cell. Longev. (2020), https://doi.org/10.1155/2020/6375938.
[6] C. Gu, L. Li, Y. Huang, D. Qian, W. Liu, C. Zhang, Y. Luo, Z. Zhou, F. Kong, X. Zhao, H. Liu, P. Gao, J. Chen, G. Yin, Salidroside ameliorates mitochondria-dependent neuronal apoptosis after spinal cord ischemia-reperfusion injury partially through inhibiting oxidative stress and promoting mitophagy, Oxid. Med. Cell. Longev. (2020), https://doi.org/10.1155/2020/3549704.
[7] E. Simmons, N. Scholpa, R. Schnellmann, Mitochondrial biogenesis as a therapeutic target for traumatic and neurodegenerative cns diseases, Exp. Neurol. (2020), https://doi.org/10.1016/j.expneurol.2020.113309.
[8] E. Fang, Y. Hou, S. Lautrup, M. Jensen, B. Yang, T. SenGupta, D. Caponio, R. Khezri, T. Demarest, Y. Aman, D. Figueroa, M. Morevati, H. Lee, H. Kato, H. Kassahun, J. Lee, D. Filippelli, M. Okur, A. Mangerich, D. Croteau, Y. Maezawa, C. Lyssiotis, J. Tao, K. Yokote, T. Rusten, M. Mattson, H. Jasper, H. Nilsen, V. Bohr, Nad augmentation restores mitophagy and limits accelerated aging in werner syndrome, Nat. Commun. (2019), https://doi.org/10.1038/s41467-019-13172-8.
[9] Q. Li, S. Gao, Z. Kang, M. Zhang, X. Zhao, Y. Zhai, J. Huang, G. Yang, W. Sun, J. Wang, Rapamycin enhances mitophagy and attenuates apoptosis after spinal

ischemia-reperfusion injury, Front. Neurosci. (2018), https://doi.org/10.3389/fnins.2018.00865.
[10] Y. Mao, J. Du, X. Chen, A. Al Mamun, L. Cao, Y. Yang, J. Mubwandarikwa, M. Zaeem, W. Zhang, Y. Chen, Y. Dai, J. Xiao, K. Ye, Maltol promotes mitophagy and inhibits oxidative stress via the nrf2/pink1/parkin pathway after spinal cord injury, Oxid. Med. Cell. Longev. (2022), https://doi.org/10.1155/2022/1337630.
[11] Q. Meng, Z. Chen, Q. Gao, L. Hu, Q. Li, S. Li, L. Cui, Z. Feng, X. Zhang, S. Cui, H. Zhang, Rosiglitazone ameliorates spinal cord injury inhibiting mitophagy and inflammation of neural stem cells, Oxid. Med. Cell. Longev. (2022), https://doi.org/10.1155/2022/5583512.
[12] L. Yang, M. Tsai, S. Juan, S. Chang, C. Yu, J. Lin, K. Johnson, H. Lim, Y. Fann, Y. Lee, Exerting the appropriate application of methylprednisolone in acute spinal cord injury based on time course transcriptomics analysis, Int. J. Mol. Sci. (2021), https://doi.org/10.3390/ijms222313024.
[13] T. Barrett, D. Troup, S. Wilhite, P. Ledoux, D. Rudnev, C. Evangelista, I. Kim, A. Soboleva, M. Tomashevsky, R. Edgar, Ncbi geo: mining tens of millions of expression profiles–database and tools update, Nucleic Acids Res. (2007), https://doi.org/10.1093/nar/gkl887.
[14] D. Szklarczyk, A. Gable, D. Lyon, A. Junge, S. Wyder, J. Huerta-Cepas, M. Simonovic, N. Doncheva, J. Morris, P. Bork, L. Jensen, C. Mering, String v11: protein-protein association networks with increased coverage, supporting functional discovery in genome-wide experimental datasets, Nucleic Acids Res. (2019), https://doi.org/10.1093/nar/gky1131.
[15] G. Stelzer, N. Rosen, I. Plaschkes, S. Zimmerman, M. Twik, S. Fishilevich, T. Stein, R. Nudel, I. Lieder, Y. Mazor, S. Kaplan, D. Dahary, D. Warshawsky, Y. Guan-Golan, A. Kohn, N. Rappaport, M. Safran, D. Lancet, The genecards suite: from gene data mining to disease genome sequence analyses, Curr. Prot. Bioinform. (2016), https://doi.org/10.1002/cpbi.5.
[16] M. Ashburner, C. Ball, J. Blake, D. Botstein, H. Butler, J. Cherry, A. Davis, K. Dolinski, S. Dwight, J. Eppig, M. Harris, D. Hill, L. Issel-Tarver, A. Kasarskis, S. Lewis, J. Matese, J. Richardson, M. Ringwald, G. Rubin, G. Sherlock, Gene ontology: tool for the unification of biology. The gene ontology consortium, Nat. Genet. (2000), https://doi.org/10.1038/75556.
[17] E. Altermann, T. Klaenhammer, Pathwayvoyager: pathway mapping using the kyoto encyclopedia of genes and genomes (kegg) database, BMC Genom. (2005), https://doi.org/10.1186/1471-2164-6-60.
[18] G. Yu, L. Wang, Y. Han, Q. He, Clusterprofiler: an r package for comparing biological themes among gene clusters, OMICS A J. Integr. Biol. (2012), https://doi.org/10.1089/omi.2011.0118.
[19] A. Subramanian, P. Tamayo, V. Mootha, S. Mukherjee, B. Ebert, M. Gillette, A. Paulovich, S. Pomeroy, T. Golub, E. Lander, J. Mesirov, Gene set enrichment analysis: a knowledge-based approach for interpreting genome-wide expression profiles, in: Proceedings of the National Academy of Sciences of the United States of America, 2005, https://doi.org/10.1073/pnas.0506580102.
[20] A. Liberzon, C. Birger, H. Thorvaldsdóttir, M. Ghandi, J. Mesirov, P. Tamayo, The molecular signatures database (msigdb) hallmark gene set collection, Cell Syst. (2015), https://doi.org/10.1016/j.cels.2015.12.004.
[21] P. Langfelder, S. Horvath, Wgcna: an r package for weighted correlation network analysis, BMC Bioinf. (2008), https://doi.org/10.1186/1471-2105-9-559.
[22] M. Smoot, K. Ono, J. Ruscheinski, P. Wang, T. Ideker, Cytoscape 2.8: new features for data integration and network visualization, in: Bioinformatics (Oxford, England), 2011, https://doi.org/10.1093/bioinformatics/btq675.
[23] C. Chin, S. Chen, H. Wu, C. Ho, M. Ko, C. Lin, Cytohubba: identifying hub objects and sub-networks from complex interactome, BMC Syst. Biol. (2014), https://doi.org/10.1186/1752-0509-8-s4-s11.
[24] G. Yu, Gene ontology semantic similarity analysis using gosemsim, in: Methods in Molecular Biology (Clifton, N.J.), 2020, https://doi.org/10.1007/978-1-0716-0301-7_11.
[25] R. Mazumder, T. Hastie, The graphical lasso: new insights and alternatives, Electr. J. Stat. (2012), https://doi.org/10.1214/12-ejs740.
[26] S. Engebretsen, J. Bohlin, Statistical predictions with glmnet, Clin. Epigenet. (2019), https://doi.org/10.1186/s13148-019-0730-1.
[27] X. Robin, N. Turck, A. Hainard, N. Tiberti, F. Lisacek, J. Sanchez, M. Müller, Proc: an open-source package for r and s+ to analyze and compare roc curves, BMC Bioinf. (2011), https://doi.org/10.1186/1471-2105-12-77.
[28] E. Lock, D. Dunson, Bayesian consensus clustering, in: Bioinformatics (Oxford, England), 2013, https://doi.org/10.1093/bioinformatics/btt425.
[29] M. Wilkerson, D. Hayes, Consensusclusterplus: a class discovery tool with confidence assessments and item tracking, Bioinformatics (2010), https://doi.org/10.1093/bioinformatics/btq170. Oxford, England.
[30] B. Chen, M. Khodadoust, C. Liu, A. Newman, A. Alizadeh, Profiling tumor infiltrating immune cells with cibersort, Methods Mol. Biol. (2018), https://doi.org/10.1007/978-1-4939-7493-1_12.
[31] H. Huang, Y. Lin, J. Li, K. Huang, S. Shrestha, H. Hong, Y. Tang, Y. Chen, C. Jin, Y. Yu, J. Xu, Y. Li, X. Cai, Z. Zhou, X. Chen, Y. Pei, L. Hu, J. Su, S. Cui, F. Wang, Y. Xie, S. Ding, M. Luo, C. Chou, N. Chang, K. Chen, Y. Cheng, X. Wan, W. Hsu, T. Lee, F. Wei, H. Huang, Mirtarbase 2020: updates to the experimentally validated microrna-target interaction database, Nucleic Acids Res. (2020), https://doi.org/10.1093/nar/gkz896.
[32] D. Karagkouni, M. Paraskevopoulou, S. Chatzopoulos, I. Vlachos, S. Tastsoglou, I. Kanellos, D. Papadimitriou, I. Kavakiotis, S. Maniou, G. Skoufos, T. Vergoulis, T. Dalamagas, A. Hatzigeorgiou, Diana-tarbase v8: a decade-long collection of experimentally supported mirna-gene interactions, Nucleic Acids Res. (2018), https://doi.org/10.1093/nar/gkx1141.
[33] J. Li, S. Liu, H. Zhou, L. Qu, J. Yang, Starbase v2.0: decoding mirna-cerna, mirna-ncrna and protein-rna interaction networks from large-scale clip-seq data, Nucleic Acids Res. (2014), https://doi.org/10.1093/nar/gkt1248.
[34] G. Zhou, O. Soufan, J. Ewald, R. Hancock, N. Basu, J. Xia, Networkanalyst 3.0: a visual analytics platform for comprehensive gene expression profiling and meta-analysis, Nucleic Acids Res. (2019), https://doi.org/10.1093/nar/gkz240.
[35] S. Freshour, S. Kiwala, K. Cotto, A. Coffman, J. McMichael, J. Song, M. Griffith, O. Griffith, A. Wagner, Integration of the drug-gene interaction database (dgidb 4.0) with open crowdsource efforts, Nucleic Acids Res. (2021), https://doi.org/10.1093/nar/gkaa1084.
[36] Q. Deng, L. Ma, Y. Yang, T. Chen, L. Zhan, Q. He, Y. Jiang, L. Ma, Effect of electroacupuncture stimulation on proliferation and differentiation of endogenous neural stem cells in rats with spinal cord injury, Mol. Neurobiol. (2023), https://doi.org/10.1007/s12035-023-03577-4.
[37] R. Kumar, J. Lim, R. Mekary, A. Rattani, M. Dewan, S. Sharif, E. Osorio-Fonseca, K. Park, Traumatic spinal injury: global epidemiology and worldwide volume, World Neurosurg. (2018), https://doi.org/10.1016/j.wneu.2018.02.033.
[38] S. Ni, B. Yang, L. Xia, H. Zhang, Aezh2 mediates mir-146a-5p/hif-1 to alleviate inflammation and glycolysis after acute spinal cord injury, Mediat. Inflamm. (2021), https://doi.org/10.1155/2021/5591582.
[39] Z. Sun, F. Liang, J. Yang, Y. Hai, Q. Su, X. Liu, The mechanism by which hyperbaric oxygen treatment alleviates spinal cord injury: genome-wide transcriptome analysis, Neur. Regenerat. Res. (2022), https://doi.org/10.4103/1673-5374.339498.
[40] C. Zu, J. Li, X. He, L. Ji, X. Li, Identification of a circrna-mediated comprehensive cerna network in spinal cord injury pathogenesis, in: Experimental Biology and Medicine (Maywood, N.J.), 2022, https://doi.org/10.1177/15353702221082929.
[41] F. Wang, C. Xu, E. Reece, X. Li, Y. Wu, C. Harman, J. Yu, D. Dong, C. Wang, P. Yang, J. Zhong, P. Yang, Protein kinase c-alpha suppresses autophagy and induces neural tube defects via mir-129-2 in diabetic pregnancy, Nat. Commun. (2017), https://doi.org/10.1038/ncomms15182.
[42] M. Abudureyimu, W. Yu, R. Cao, Y. Zhang, H. Liu, H. Zheng, Berberine promotes cardiac function by upregulating pink1/parkin-mediated mitophagy in heart failure, Front. Physiol. (2020), https://doi.org/10.3389/fphys.2020.565751.
[43] C. Wu, H. Chen, R. Zhuang, H. Zhang, Y. Wang, X. Hu, Y. Xu, J. Li, Y. Li, X. Wang, H. Xu, W. Ni, K. Zhou, Betulinic acid inhibits pyroptosis in spinal cord injury by augmenting autophagy via the ampk-mtor-tfeb signaling pathway, Int. J. Biol. Sci. (2021), https://doi.org/10.7150/ijbs.57825.
[44] S. Mamidi, A. Healey, P. Huang, J. Grimwood, J. Jenkins, K. Barry, A. Sreedasyam, S. Shu, J. Lovell, M. Feldman, J. Wu, Y. Yu, C. Chen, J. Johnson, H. Sakakibara, T. Kiba, T. Sakurai, R. Tavares, D. Nusinow, I. Baxter, J. Schmutz, T. Brutnell, E. Kellogg, A genome resource for green millet setaria viridis enables discovery of agronomically valuable loci, Nat. Biotechnol. (2020), https://doi.org/10.1038/s41587-020-0681-2.
[45] L. Thompson, K. Rutherford, C. Lepage, K. McManus, Aberrant skp1 expression: diverse mechanisms impacting genome and chromosome stability, Front. Cell Dev. Biol. (2022), https://doi.org/10.3389/fcell.2022.859582.
[46] L. Dabool, K. Hakim-Mishnaevski, L. Juravlev, N. Flint-Brodsly, S. Mandel, E. Kurant, Drosophila skp1 homologue skpa plays a neuroprotective role in adult brain, iScience (2020), https://doi.org/10.1016/j.isci.2020.101375.
[47] M. He, M. Chaurushiya, J. Webster, S. Kummerfeld, R. Reja, S. Chaudhuri, Y. Chen, Z. Modrusan, B. Haley, D. Dugger, J. Eastham-Anderson, S. Lau, A. Dey, R. Caothien, M. Roose-Girma, K. Newton, V. Dixit, Intrinsic Apoptosis Shapes the Tumor Spectrum Linked to Inactivation of the Deubiquitinase Bap1, Science, New York, N.Y., 2019, https://doi.org/10.1126/science.aav4902.
[48] S. Lee, D. Lee, M. Kang, S. Kim, S. Kwon, H. Lee, H. Seo, P. Kaushal, N. Lee, H. Kim, C. Lee, J. Kwon, Bap1 promotes the repair of uv-induced DNA damage via parp1-mediated recruitment to damage sites and control of activity and stability, Cell Death Differ. (2022), https://doi.org/10.1038/s41418-022-01024-w.
[49] A. Bononi, H. Yang, C. Giorgi, S. Patergnani, L. Pellegrini, M. Su, G. Xie, V. Signorato, S. Pastorino, P. Morris, G. Sakamoto, S. Kuchay, G. Gaudino, H. Pass, A. Napolitano, P. Pinton, W. Jia, M. Carbone, Germline bap1 mutations induce a warburg effect, Cell Death Differ. (2017), https://doi.org/10.1038/cdd.2017.95.
[50] Z. Xiong, P. Xia, X. Zhu, J. Geng, S. Wang, B. Ye, X. Qin, Y. Qu, L. He, D. Fan, Y. Du, Y. Tian, Z. Fan, Glutamylation of deubiquitinase bap1 controls self-renewal of hematopoietic stem cells and hematopoiesis, J. Exp. Med. (2020), https://doi.org/10.1084/jem.20190974.
[51] J. Kuznetsov, T. Aguero, D. Owens, S. Kurtenbach, M. Field, M. Durante, D. Rodriguez, M. King, J. Harbour, Bap1 regulates epigenetic switch from pluripotency to differentiation in developmental lineages giving rise to bap1-mutant cancers, Sci. Adv. (2019), https://doi.org/10.1126/sciadv.aax1738.
[52] T. Jones, Lymphocytes and autoimmunity after spinal cord injury, Exp. Neurol. (2014), https://doi.org/10.1016/j.expneurol.2014.03.003.
[53] T. Gao, F. Huang, Y. Xie, W. Wang, L. Wang, D. Mu, Y. Cui, B. Wang, Dynamic changes in the systemic immune responses of spinal cord injury model mice, Neur. Regenerat. Res. (2021), https://doi.org/10.4103/1673-5374.290910.
[54] T. Arenzana, S. Lianoglou, A. Seki, C. Eidenschenk, T. Cheung, D. Seshasayee, T. Hagenbeek, A. Sambandam, R. Noubade, I. Peng, J. Lesch, J. DeVoss, X. Wu, W. Lee, P. Caplazi, J. Webster, J. Liu, V. Pham, D. Arnott, J. Lill, Z. Modrusan, A. Dey, S. Rutz, Tumor suppressor bap1 is essential for thymic development and proliferative responses of t lymphocytes, Sci. Immunol. (2018), https://doi.org/10.1126/sciimmunol.aal1953.
[55] J. Jeong, I. Jung, J. Kim, S. Jeon, D. Hyeon, H. Min, B. Kang, J. Nah, D. Hwang, S. Um, M. Ko, R. Seong, Bap1 shapes the bone marrow niche for lymphopoiesis by fine-tuning epigenetic profiles in endosteal mesenchymal stromal cells, Cell Death Differ. (2022), https://doi.org/10.1038/s41418-022-01006-y.

[56] U. Sharma, T. Barwal, A. Khandelwal, M. Rana, A. Rana, K. Singh, A. Jain, Circulating long non-coding rnas linc00324 and loc100507053 as potential liquid biopsy markers for esophageal squamous cell carcinoma: a pilot study, Front. Oncol. (2022), https://doi.org/10.3389/fonc.2022.823953.
[57] Y. Chen, Y. Wu, R. Chen, C. Xu, Q. Chen, Lncrna linc00324 is upregulated in intervertebral disk degeneration and upregulates fasl in nucleus pulposus cells, Mol. Cell. Biochem. (2021), https://doi.org/10.1007/s11010-021-04058-9.
[58] C. Xie, B. Zhu, J. Gu, M. Sun, The correlation of lncrna snhg16 with inflammatory cytokines, adhesion molecules, disease severity, and prognosis in acute ischemic stroke patients, J. Clin. Lab. Anal. (2022), https://doi.org/10.1002/jcla.24439.
[59] H. Liu, B. Chen, Q. Zhu, Long non-coding rna snhg16 reduces hydrogen peroxide-induced cell injury in pc-12 cells by up-regulating microrna-423-5p, Artif. Cells, Nanomed. Biotechnol. (2019), https://doi.org/10.1080/21691401.2019.1600530.
[60] H. Teng, M. Li, L. Qian, H. Yang, M. Pang, Long non-coding rna snhg16 inhibits the oxygen-glucose deprivation and reoxygenation-induced apoptosis in human brain microvascular endothelial cells by regulating mir-15a-5p/bcl-2, Mol. Med. Rep. (2020), https://doi.org/10.3892/mmr.2020.11385.
[61] X. Cao, J. Ma, S. Li, Mechanism of lncrna snhg16 in oxidative stress and inflammation in oxygen-glucose deprivation and reoxygenation-induced sk-n-sh cells, Bioengineered (2022), https://doi.org/10.1080/21655979.2022.2026861.
[62] E. Rampazzo, L. Manfreda, S. Bresolin, A. Cani, E. Mariotto, R. Bortolozzi, A. Della Puppa, G. Viola, L. Persano, Histone deacetylase inhibitors impair glioblastoma cell motility and proliferation, Cancers (2022), https://doi.org/10.3390/cancers14081897.
[63] M. Melica, G. Antonelli, R. Semeraro, M. Angelotti, G. Lugli, S. Landini, F. Ravaglia, G. Regina, C. Conte, L. De Chiara, A. Peired, B. Mazzinghi, M. Donati, A. Molli, S. Steiger, A. Magi, N. Bartalucci, V. Raglianti, F. Guzzi, L. Maggi, F. Annunziato, A. Burger, E. Lazzeri, H. Anders, L. Lasagni, P. Romagnani, Differentiation of crescent-forming kidney progenitor cells into podocytes attenuates severe glomerulonephritis in mice, Sci. Transl. Med. (2022), https://doi.org/10.1126/scitranslmed.abg3277.
[64] A. Schoeller, K. Karki, A. Jayaraman, R. Chapkin, S. Safe, Short chain fatty acids exhibit selective estrogen receptor downregulator (serd) activity in breast cancer, Am. J. Cancer Res. 12 (7) (2022) 3422–3436.
[65] N. Ranallo, A. Iamurri, F. Foca, C. Liverani, A. De Vita, L. Mercatali, C. Calabrese, C. Spadazzi, C. Fabbri, D. Cavaliere, R. Galassi, S. Severi, M. Sansovini, A. Tartaglia, F. Pieri, L. Crudi, D. Bianchini, D. Barone, G. Martinelli, G. Frassineti, T. Ibrahim, L. Calabrò, R. Berardi, A. Bongiovanni, Prognostic and predictive role of body composition in metastatic neuroendocrine tumor patients treated with everolimus: a real-world data analysis, Cancers (2022), https://doi.org/10.3390/cancers14133231.
[66] T. Powles, M. Lackner, S. Oudard, B. Escudier, C. Ralph, J. Brown, R. Hawkins, D. Castellano, B. Rini, M. Staehler, A. Ravaud, W. Lin, B. O'Keeffe, Y. Wang, S. Lu, J. Spoerke, L. Huw, M. Byrtek, R. Zhu, J. Ware, R. Motzer, Randomized open-label phase ii trial of apitolisib (gdc-0980), a novel inhibitor of the pi3k/mammalian target of rapamycin pathway, versus everolimus in patients with metastatic renal cell carcinoma, J. Clin. Oncol. : Off. J. Am. Soc. Clin. Oncol. (2016), https://doi.org/10.1200/jco.2015.64.8808.
[67] S. Dolly, C. Migali, N. Tunariu, C. Della-Pepa, S. Khakoo, S. Hazell, J. de Bono, S. Kaye, S. Banerjee, Indolent peritoneal mesothelioma: pi3k-mtor inhibitors as a novel therapeutic strategy, ESMO Open (2017), https://doi.org/10.1136/esmoopen-2016-000101.
[68] E. Tolstik, M. Gongalsky, J. Dierks, T. Brand, M. Pernecker, N. Pervushin, D. Maksutova, K. Gonchar, J. Samsonova, G. Kopeina, V. Sivakov, L. Osminkina, K. Lorenz, Raman and fluorescence micro-spectroscopy applied for the monitoring of sunitinib-loaded porous silicon nanocontainers in cardiac cells, Front. Pharmacol. (2022), https://doi.org/10.3389/fphar.2022.962763.
[69] M. Cahuzac, B. Péant, A. Mes-Masson, F. Saad, Development of olaparib-resistance prostate cancer cell lines to identify mechanisms associated with acquired resistance, Cancers (2022), https://doi.org/10.3390/cancers14163877.